Electronic Supplementary Information

Methane-Trapping Metal-Organic Frameworks with An Aliphatic Ligand for Efficient CH_4/N_2 Separation

Miao Chang[‡ a], Yingjie Zhao[‡ a], Dahuan Liu [*a], Jiangfeng Yang [b], Jinping Li [b] and Chongli Zhong [a,c]

[a] Beijing Advanced Innovation Center for Soft Matter Science and Engineering, Beijing University of Chemical Technology, Beijing 100029, China
[b] Research Institute of Special Chemicals, Taiyuan University of Technology, Taiyuan 030024, Shanxi China
[c] State Key Laboratory of Separation Membranes and Membrane Processes, Tianjin Polytechnic University, Tianjin 300387, China

Table of Contents

1. Experimental Section

1.1 Materials

All chemicals reagents and solvents are commercially available and directly used without further purification. Metal salts and the organic ligand were purchased from J&K Scientific Ltd. Methanol and N, N-dimethylformamide (DMF) were obtained from TCI.

1.2 Instrumentation

Powder X-ray diffraction (PXRD) was measured by D8 Advance X diffractometer equipped with a Cu sealed tube (λ = 1.54178 Å). The specific surface area, pore size and adsorption isotherms were measured on a Quantachrome Autosorb-IQ instrument. The FT-IR spectroscopy data was obtained by Nicolet 6700 FTIR instrument. The morphologies of materials were confirmed by Field-Emission Scanning Electron Microscopy (FESEM, Gemini 300). The lattice fringe of the material was obtained by high-resolution TEM (HRTEM, H-9500). Thermogravimetric analysis was performed by GA Q50 from 298 K to 1073 K with air atmosphere and the heating rate was 5 K/min. The concentration of the effluent gas from column determined by a gas chromatograph (Shimadzu, GC-2014C) for breakthrough experiment.

1.3 Synthesis of MOFs

Al-CDC was synthesized using the modified method on the basis of the previously reported one in literature.[1] $AlCl_3$•$6H_2O$ (1.448 g, 6 mmol), H_2CDC (1.002 g, 6 mmol) were mixed with DMF (32 ml) and distilled water (8 ml) in a round bottom flask (50 ml) at 403 K for about 5 minutes with stirred, then the white product was obtained by centrifugation. After being washed with DMF and acetone several times, the material was dried in the vacuum oven at 403 K for 12 h.

Cu-CDC was synthesized according to the previously reported method in literature.[2] $Cu(NO_3)_2$•$6H_2O$ (2.95 g), H_2CDC (2.15 g) and DMF (150 g) were placed in a 100 ml Teflon-lined steel autoclave, followed by being transferred into oven and then heated to 358 K for 3 days. The obtained blue crystals were filtered and washed several times with DMF and methanol. Finally, the material was dried in the vacuum oven at 403 K for 12 h.

In-CDC was synthesized according to the previously reported method in literature.[3] $InCl_3$•$4H_2O$ (350 mg, 1.19 mmol) and H_2CDC (420 mg, 2.45 mmol) were mixed in acetonitrile (14 ml) and distilled water (28 ml). Then, the mixture was put in a 100 ml Teflon-lined stainless steel vessel autoclave and heated to 433 K for 3 days. The white crystals were obtained by centrifugation, washed by distilled water and acetone several times. Finally, the material was placed in a vacuum oven at 403 K for 12 h.

1.4 Gas adsorption measurement

CH_4 and N_2 adsorption isotherms at different temperatures as well as cycle experiment of CH_4 adsorption were measured by a Quantachrome Autosorb-IQ instrument. About 800 mg sample was outgassed at 473 K for 12 h before gas adsorption measurement.

1.5 Breakthrough measurement

3.50 g sample was filled in the column (10 × 150 mm) and purged with helium (25 ml/min) at 473 K for 6 h until the device was cooled down to room temperature. Then the equimolar mixture of CH_4 and N_2 was flowed into the column with the total flow rate of 10.0 ml/min. The effluent gas from the column was detected by gas chromatograph (Shimadzu, GC-2014C). The uptake capacity (q_i) were determined using the following equation:[4]

$$q_i = \frac{C_i V}{22.4 \times m} \times \int_0^t (1 - \frac{F}{F_0}) dt$$

where q_i refers to the uptake capacity of gas *i* (cm^3/g), C_i represents the initial feed gas concentration, V is the volumetric feed flow rate (cm^3/min), t is the adsorption time (min), F_0 and F are the influent and effluent gas molar flow rates of specific gas (cm^3/min), respectively, and m is the mass of the adsorbent (g). The selectivity ($S_{breakthrough}$) of the breakthrough experiment is calculated using the following equation:[4]

$$S_{breakthrough} = \frac{q_1/y_1}{q_2/y_2}$$

where y_i is the molar fraction of gas *i* (*i* =1, 2) in the gas mixture.

1.6 Property calculations

Selectivities of the studied materials were calculated using the ideal adsorbed solution theory (IAST) according to the single component experimental isotherms data.[5] S_{ij} represents adsorption selectivity of *i* and *j* components which is defined as:

$$S_{ij} = \frac{x_i/x_j}{y_i/y_j}$$

where x_i and x_j are the gas adsorption capacities of *i* and *j* components, and y_i and y_j are gas molar fractions of *i* and *j* components, respectively.

Sorbent selection parameter (SSP) is a parameter introduced first by Yang et al.[6] and promoted by Snurr et al.[7] as an overall separation performance indicator for a cyclic pressure-swing adsorption (PSA) or vacuum-swing adsorption (VSA) process, which can be calculated as:

$$SSP = \frac{(S_{i/j}{}^{ads})^2}{(S_{i/j}{}^{des})} \times \frac{(N_i{}^{ads} - N_i{}^{des})}{(N_j{}^{ads} - N_j{}^{des})}$$

where $S_{i/j}{}^{ads}$ and $S_{i/j}{}^{des}$ are the selectivities of *i* and *j* components under adsorption and desorption conditions, and N^{ads} and N^{des} are the adsorption capacity under adsorption and desorption conditions.

1.7 Calculation of isosteric heat of adsorption

The heat of adsorption is calculated using the following equation:[8]

$$Q_{st} = \frac{RT_1T_2}{T_2 - T_1}\ln\frac{P_1}{P_2}$$

where R, P_i and T_i represent the molar gas constant (8.314 J/K/mol), the pressure of isotherm, and temperature of isotherm, respectively.

1.8 Theoretical calculations

2D potential energy distributions were calculated using a simple Monte Carlo technique in the framework of MOFs.[9] One pore was specifically divided into 20 circles and the potential energies were scanned at a certain interval along the circumference for each circle. At each point, 10^5 random orientations were generated to obtain the lowest potential energies for CH_4 or N_2 molecules. The binding energy of CH_4 or N_2 molecules with the framework was calculated by density functional theory (DFT) using applying Dmol^3 in Materials Studio. We used the generalized gradient approximation (GGA) with the Perdew-

Burke-Ernzerh of (PBE) functional for the calculations. For the purpose of expanding electronic wave functions, the double numerical plus d-functions (DND) basis set is selected. The self-consistent field (SCF) calculations are used with a convergence criterion of 10^{-6} Ha in energy. In order to accelerate the self-consistent field convergence, thermal smearing with a value of 0.005 Ha is used to orbital occupation to speed up convergence. The interaction energy between the molecule of CH_4 or N_2 and Al-CDC is defined as:

$$E_{int} = E_{gas+materials} - E_{gas} - E_{materials}$$

where E_{int} is the total energy for adsorption of CH_4 or N_2 to Al-CDC, and E_{gas} and $E_{materials}$ are the energies of gas molecule and Al-CDC, respectively.

2. Adsorption isotherms

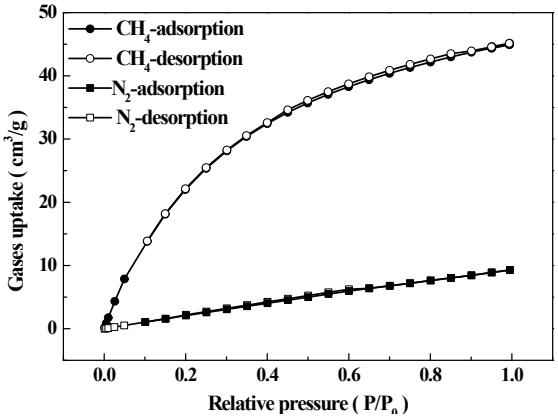

Fig. S1 Single component adsorption isotherms of CH_4 and N_2 of Al-CDC at 273 K.

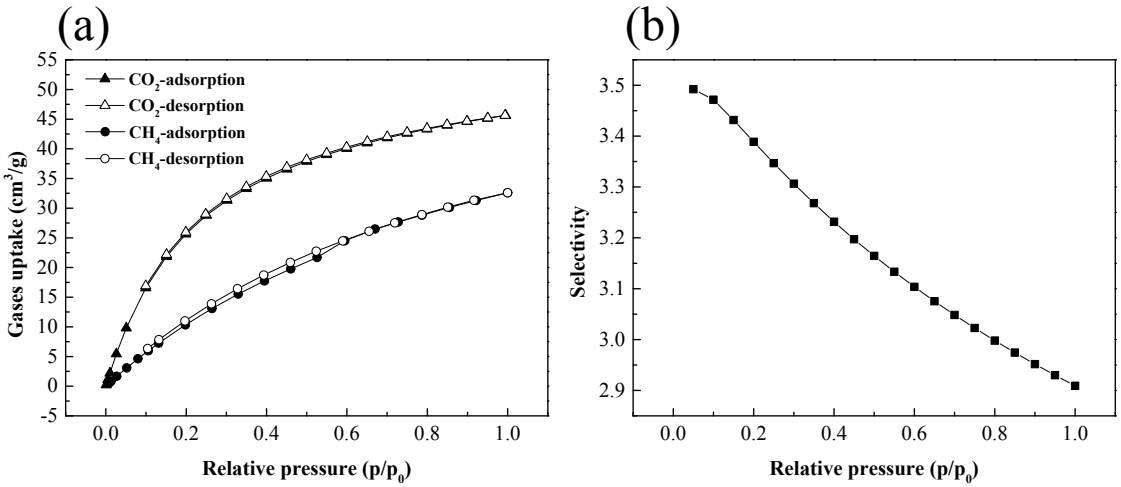

Fig. S2 (a) Single component adsorption isotherm of CO_2 and CH_4 of Al-CDC at 298 K; (b) IAST selectivity of CO_2 and CH_4 with equimolar mixtures (CO_2:CH_4 = 50:50) at 298 K.

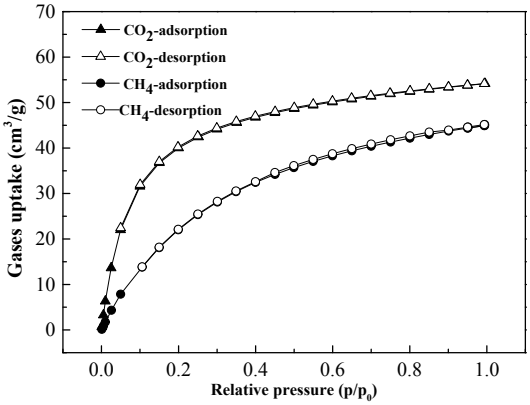

Fig. S3 Single component adsorption isotherms of CO_2 and CH_4 of Al-CDC at 273 K.

3. Calculation of selectivity

The single component isotherms for CH_4 and N_2 (CH_4 /N_2 (50/50, v/v)) at 298 K were fitted to the dual-site Langmuir equation：

$$y = \left(\frac{p_1 \times x}{p_2 + x}\right) + \left(\frac{p_3 \times x}{p_4 + x}\right)$$

The equilibrium composition of the CH_4 /N_2 mixture is 22.62: 1.73.

The calculated IAST selectivities are about 13.1-16.69 at the range of tested pressures and 13.1 at 1.0 bar.

The fitting parameters are given in **Table S1**.

Table S1 The fitting parameters by using the dual-site Langmuir equation based on the single-component isotherms data of CH_4 and N_2 in Al-CDC at 298 K.

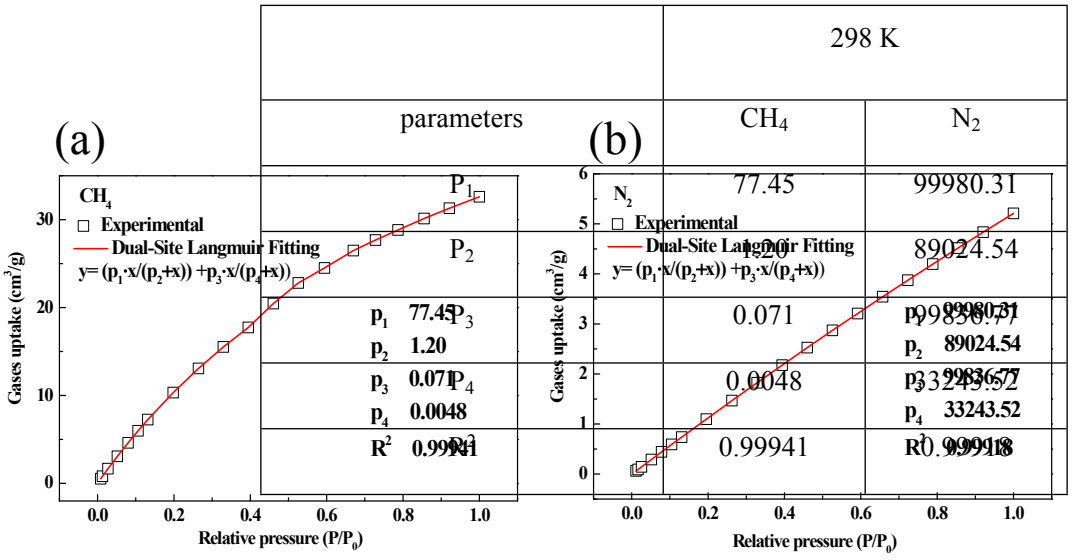

	298 K	
parameters	CH_4	N_2
P_1	77.45	99980.31
P_2	1.20	89024.54
P_3	0.071	0.0048
P_4	0.0048	33243.52
R^2	0.99941	0.99918

Fig. S4 Fitting of the CH_4 (a) and N_2 (b) adsorption data of Al-CDC at 298 K using dual-site Langmuir model.

The single component isotherms of CH_4 and N_2 (CH_4 /N_2 (50/50, v/v)) at 298 K were fitted to the Toth equation：

$$y= \frac{N_{max} \times p_1 \times x}{(1+(p_1 \times x)^{p_2})^{1/p_2}}$$

$$K_H = N_{max} \times p_1$$

$$S_{i,j} = K_{H,i} / K_{H,j}$$

The ideal selectivity is about 13.06.

The fitting parameters are given in **Table S2**.

Table S2 The fitting parameters by using the Toth equation based on the pure single component isotherms data of CH_4 and N_2 in Al-CDC at 298 K.

Parameters	CH_4	N_2
N_{max}	81.773	27.999
P_1	0.814	0.182
P_2	1.060	1.272
R^2	0.99956	0.99999

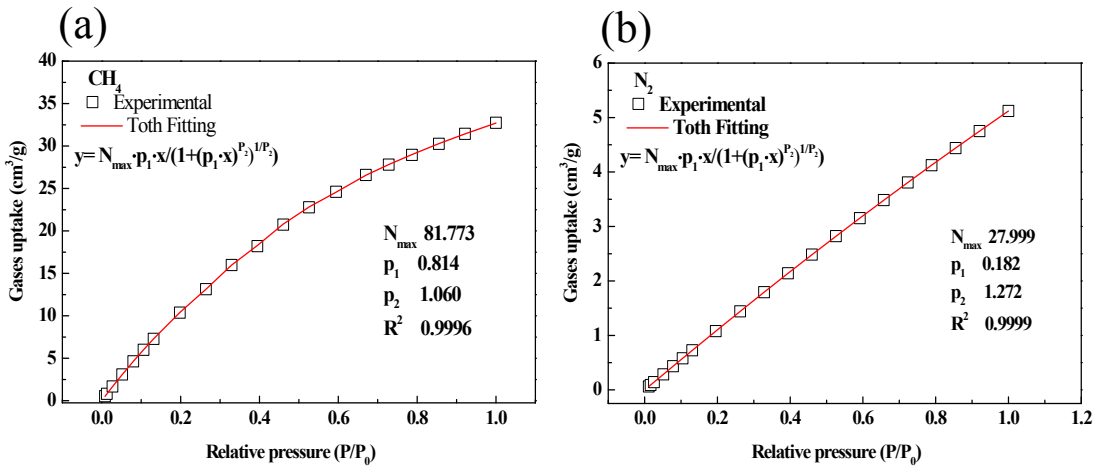

Fig. S5 Fitting of the CH_4 (a) and N_2 (b) adsorption data of Al-CDC at 298 K using Toth model.

The single component isotherms for CO_2 and CH_4 (CO_2/CH_4 (50/50, v/v)) at 298 K were fitted to the dual-site Langmuir equation：

$$y = (\frac{p_1 \times x}{p_2 + x}) + (\frac{p_3 \times x}{p_4 + x})$$

The equilibrium composition of the CO_2 /CH_4 mixture is 32.00: 11.00.

The calculated IAST selectivities are about 2.91-3.49 at the range of tested pressures and 2.91 at 1.0 bar.

The fitting parametersare given in **Table S3**.

Table S3 The fitted parameters by using the dual-site Langmuir equation based on the single-component isotherms data of CO_2 and CH_4 in Al-CDC at 298 K.

Parameters	CO_2	CH_4
P_1	54.56	77.45
P_2	0.23	1.20
P_3	99999.89	0.071
P_4	74635.85	0.0048
R^2	0.99997	0.99941

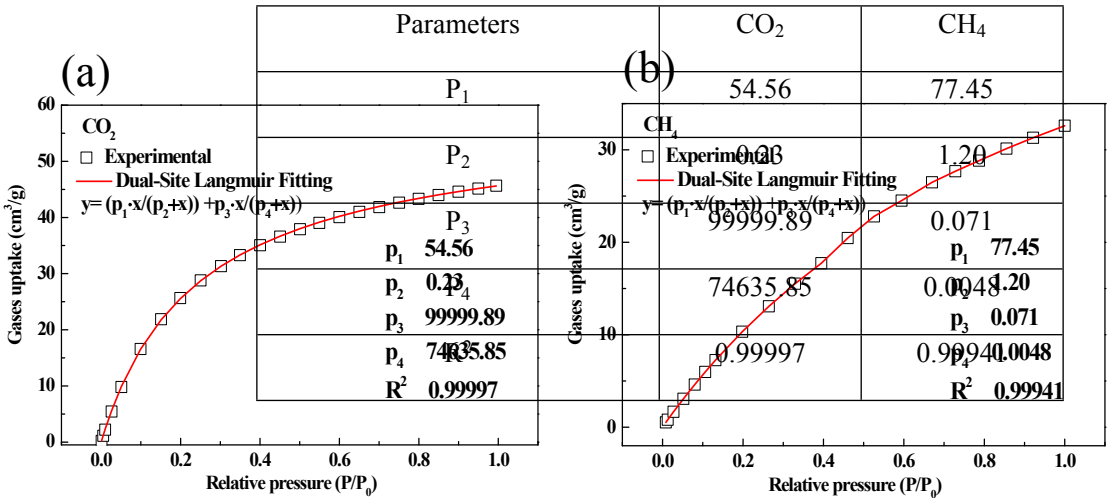

Fig. S6 Fitting of the CO_2 (a) and CH_4 (b) adsorption data of Al-CDC at 298 K using dual-site Langmuir model.

4. Characterization of MOFs

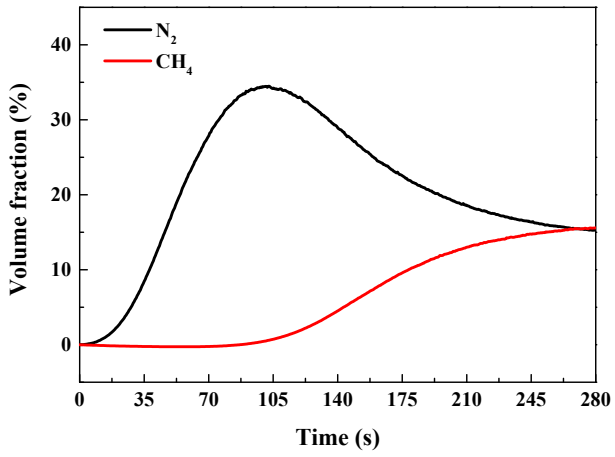

Fig. S7 Breakthrough experiment curves for the CH_4 and N_2 (10/10, v/v) binary mixture component with the presence of water (water contents: 5 %) at constant flow rate of 10 ml/min under 298 K and 1 bar

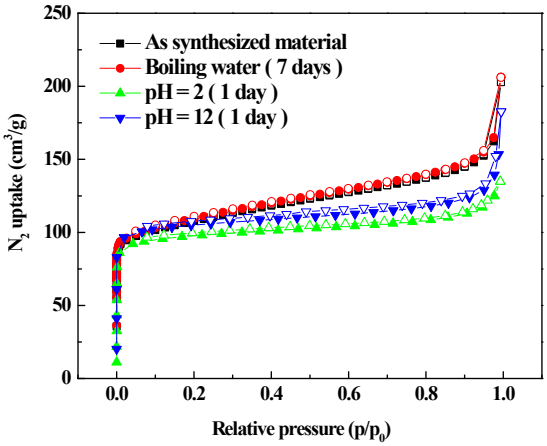

Fig. S8 N_2 adsorption isotherms at 77 K after the treatment of the material using boiling water, acid and base solution for days.

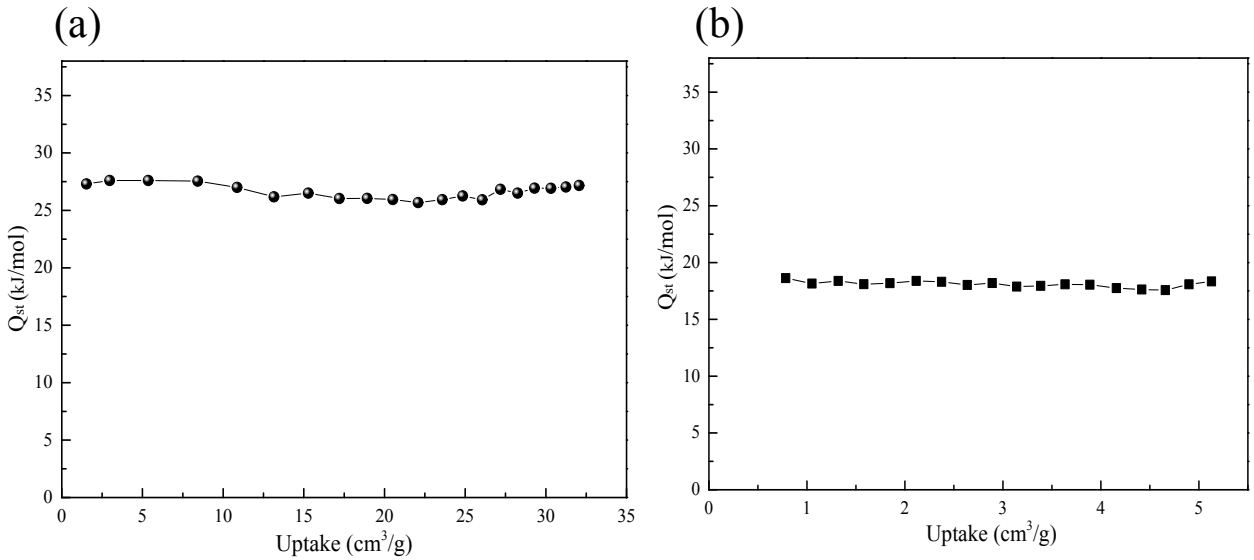

Fig. S9 Calculated isosteric heat values for CH_4 (a) and N_2 (b) of Al-CDC.

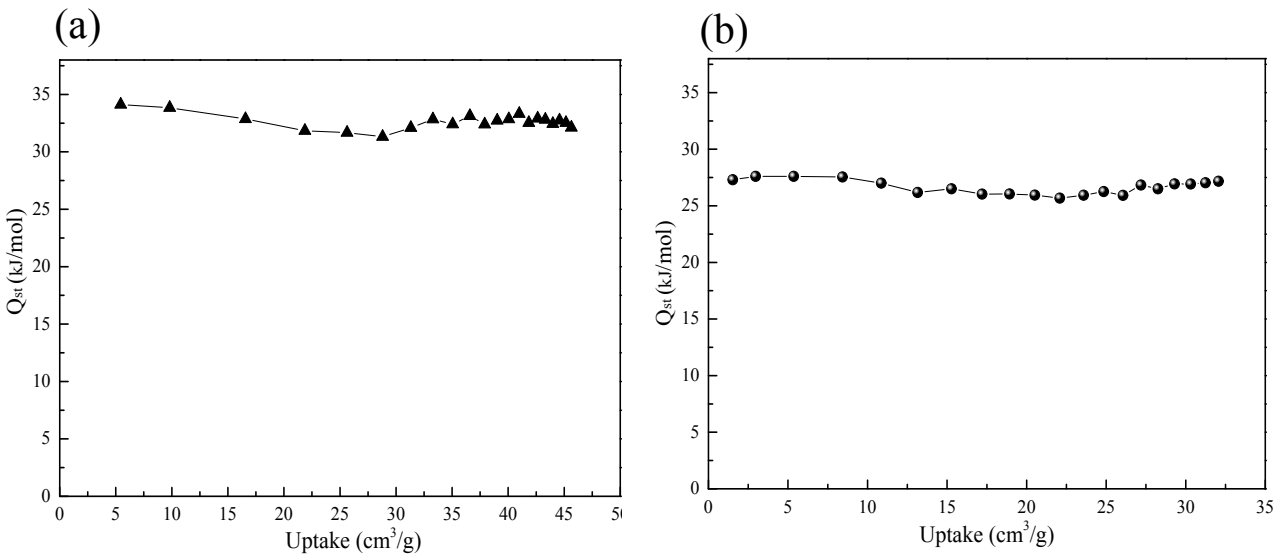

Fig. S10 Calculated isosteric heat values for CO_2 (a) and CH_4 (b) of Al-CDC.

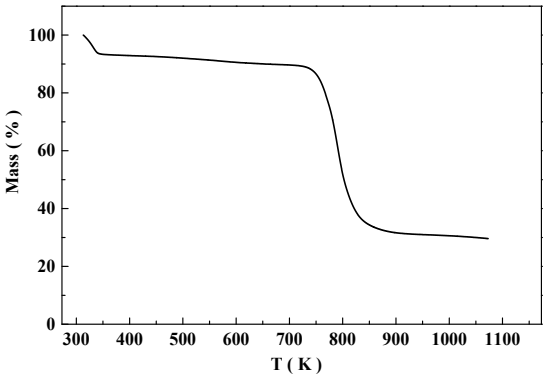

Fig. S11 TGA curve of Al-CDC.

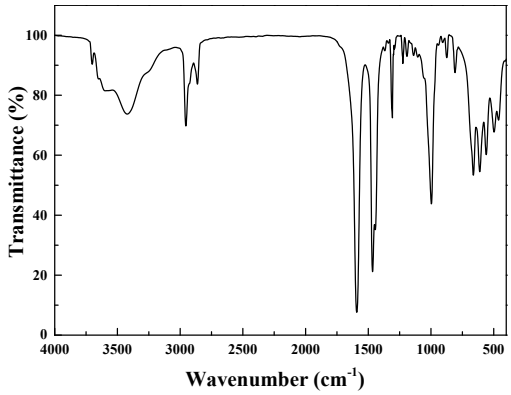

Fig. S12 FT-IR spectra of Al-CDC.

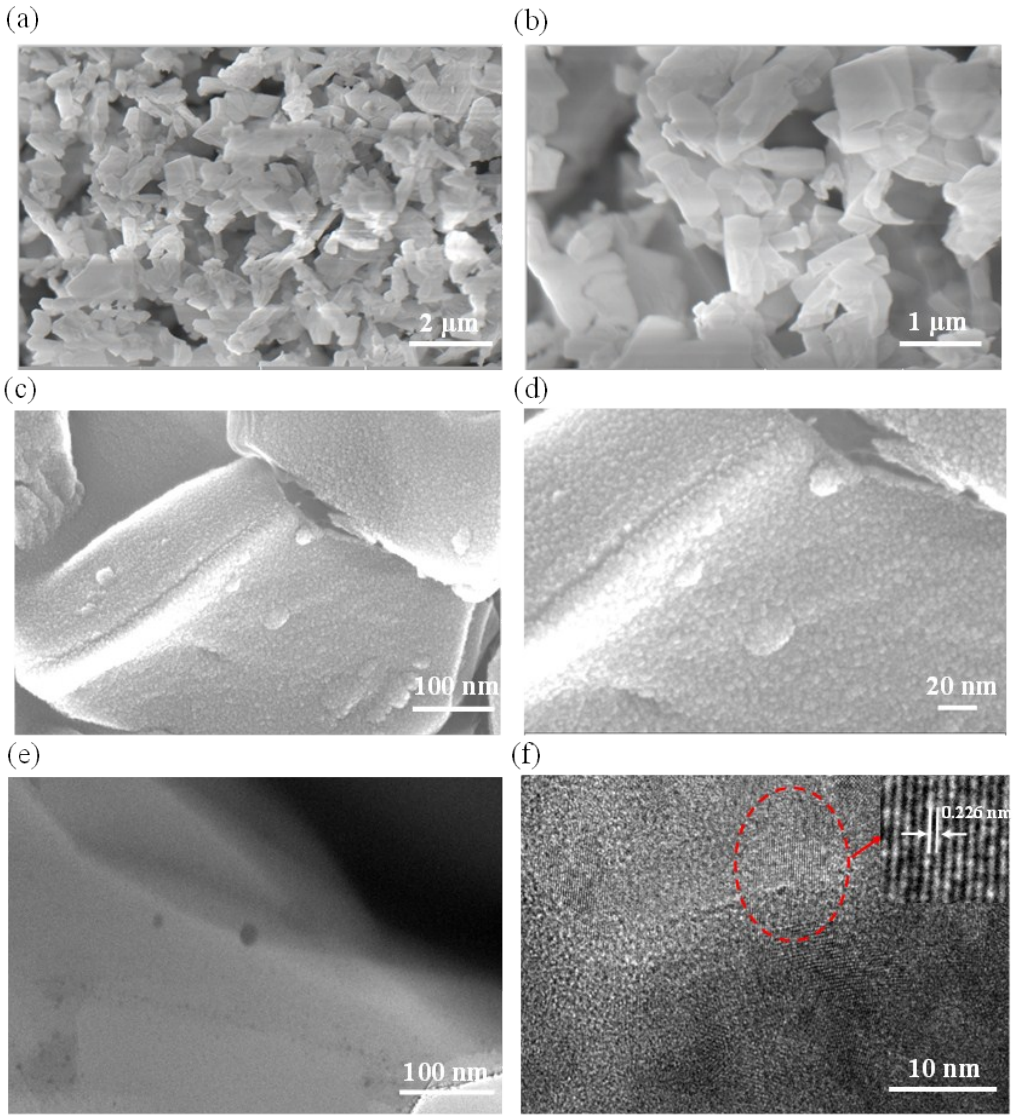

Fig. S13 FESEM images (a-d) and HRTEM images (e−f (Inset: the inverse Fourier transform of the red image area)) of Al-CDC.

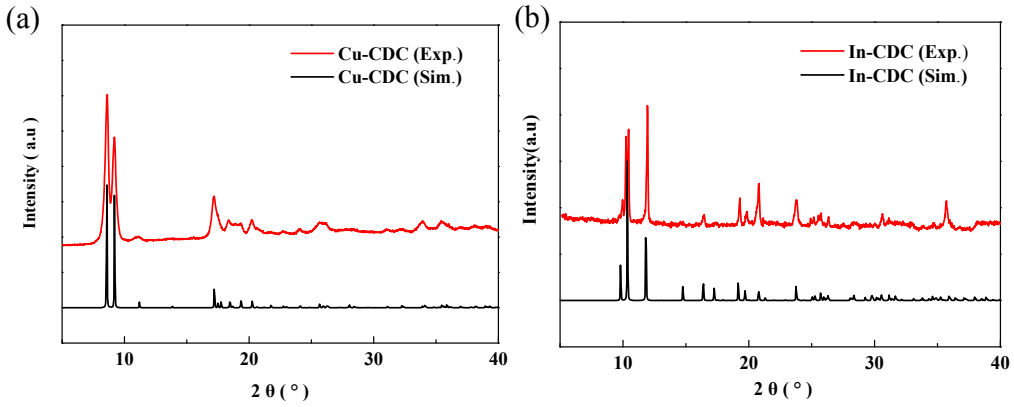

Fig. S14 Powder X-ray diffraction patterns of Cu-CDC (a) and In-CDC (b).

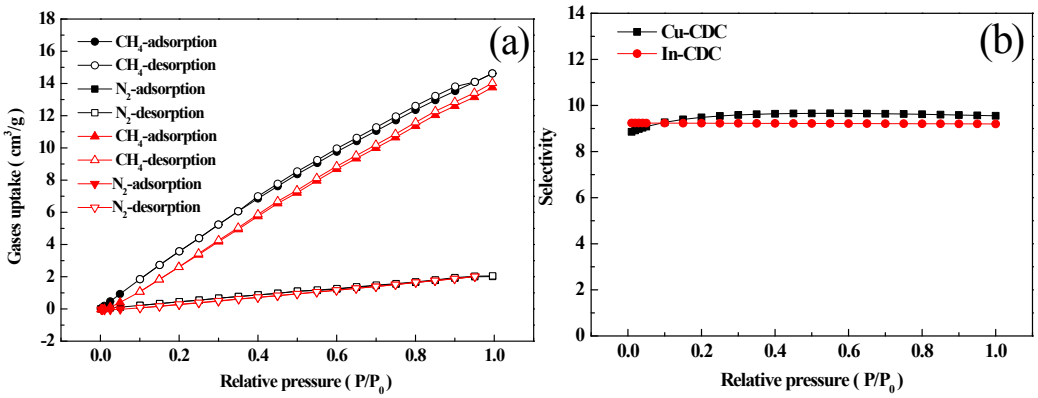

Fig. S15 (a) single component adsorption isotherm of CH_4 and N_2 for Cu-CDC (black), In-CDC (red) at 298 K, 1 bar. (b) IAST selectivity of CH_4/N_2 for Cu-CDC, In-CDC with equimolar mixtures (CH_4 : N_2 = 50 : 50) at 298 K.

Table S4 Pore size, BET surface area and Pore volume of Al-CDC

MOF	Pore size (Å)[a]	BET surface area (m^2/g)[b]	Pore volume (cm^3/g)[c]
Al-CDC	5.4	380	0.257

[a] Calculated by DFT method. [b] Calculated from N_2 adsorption isotherms at 77 K in the range of P/P_0 = 0.001− 0.05.

[c] Calculated by adsorbed amounts of N_2 at P/P_0 = 0.95.

5. Comparison with other porous materials

Table S5 Selectivity and adsorption heat of CH_4 and N_2 in different materials at 298 K and 1 bar.

Adsorbents	Selectivity for 50/50 CH_4/N_2 mixture	Q_{st} for CH_4 (kJ/mol)	Q_{st} for N_2 (kJ/mol)	Refs.
Co-MOF	12.5[a]	25.13	18.12	10
sOMC	3.5[a]			4
CTF-650	8.6[a]	27		4
Na-SAPO-34	2.6[b]	12.18	22.03	11
AC	3.85[a]			12
$[Ni_3(HCOO)_6]$	6.1[c]	24.82	19.33	12
$[Co_3(HCOO)_6]$	5.1[c]	23.03	19.7	12
Cu-BTC	3.69[c]	16.6	13.9	12
Mg-Clinoptilolite	2[c]			12
[Cu(Me-4py-trz-ia)]	4.2[a]	18	12	13
Basolite A100	3.7[a]	19	15.9	13
MOF-888	8.38[a]	26	22	14
MOF-889	6.41[a]	22	19	14
MOF-890	7[a]	23	19	14
MOF-891	7.78[a]	22	21	14
MOF-5	1.13[c]	12.2		15
MOF-177	4[c]	11.74		15
$Cu(OTf)_2$	4.8[a]	19.6	16	16
ZIF-68	3.5[a]	15.7[e]	11.9[e]	17
ZIF-69	3[a]	16.2[e]	12.8[e]	17
Ni-MOF	6[a]	22.2	18	18
ZIF-8	2.8[d]	12.4[e]	9.8[e]	19
MIL-101- Cr	2.65[a] (293 K)	15.73 (293 K)	12 (293 K)	20
Cu-MOF	6.9[a]	24	20	21
$Cu(INA)_2$	8.34[c]	17.52		22
Al-BDC	3.56[c]	18.74		22
Ni-HKUST-1	5.1[a]			23
Boron nitride	10[a]			24
$[Ni_3(HCOO)_6]$	6.18[c]			25
ATC-Cu	9.7[a]	26.8	16.0	26
ROD-8	9.1[a]	16.7		27
Zeolite 5A	0.94[c]			28
$Ni(OAc)_2L$	7[a]	26.7	20	28
Al-CDC	13.1[a]	27.5	18.6	This work
Al-CDC		26.52[e]	10.7[e]	This work
Al-CDC	13.3[c]			This work

[a] Predicted by IAST. [b] Mixture selectivity.[c] Calculated by the ratio of Henry's law constants. [d] Calculated by theoretical calculations. [e] Obtained from calculations.

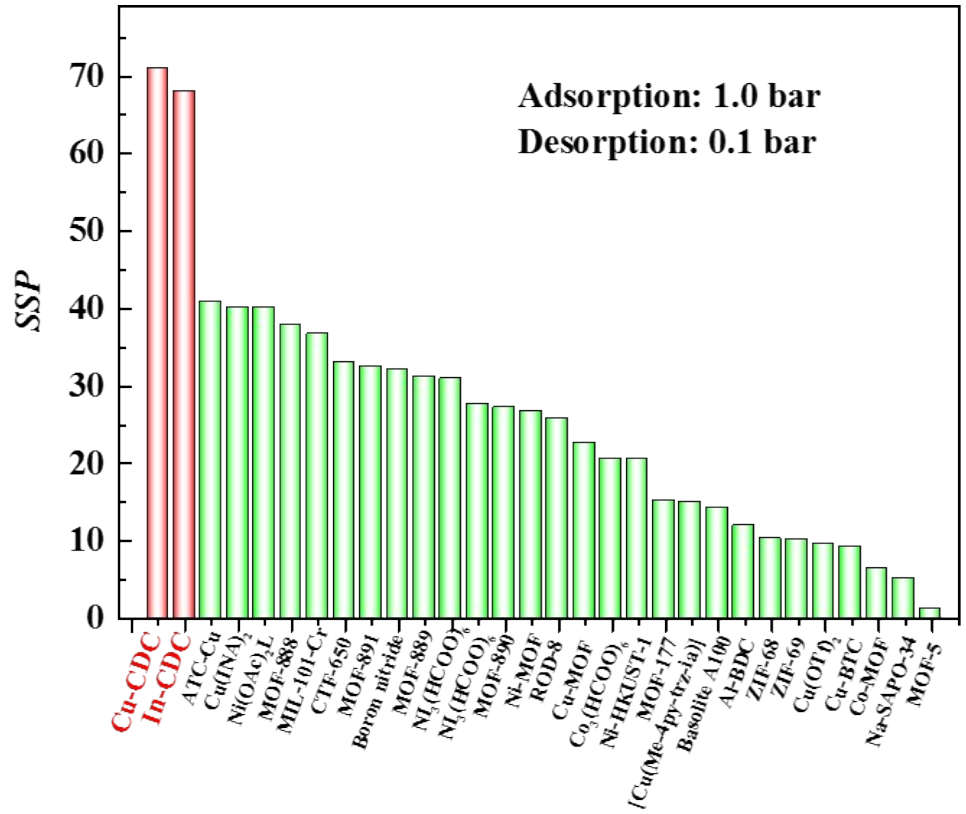

Fig. S16 Comparison of *SSP* in Cu-CDC and In-CDC with other reported porous materials.

Table S6 Uptake capacity of CH_4 and *SSP* values in different materials at 298 K and 1.0 bar.

Adsorbents	Uptake capacity of CH_4 (cm^3/g)	*SSP* value	Refs
Co-MOF	9.03	6.32[a]	10
sOMC	22.0		4
CTF-650	32.0	33[a]	4
Na-SAPO-34	13.4	5.08[b]	11
AC	5.68		12
$[Ni_3(HCOO)_6]$	17.71	27.6[c]	12
$[Co_3(HCOO)_6]$	10.98	20.6[c]	12
Cu-BTC	20.41	9.16[a]	12
Mg-Clinoptilolite			12
[Cu(Me-4py-trz-ia)]	25.09	15[a]	13
Basolite A100	16.58	14.21[a]	13
MOF-888	10.09	37.85[a]	14
MOF-889	25.98	31.15[a]	14
MOF-890	23.97	27.2[a]	14
MOF-891	29.99	32.41[a]	14
MOF-5	2.91	1.05[c]	15
MOF-177	12.61	15.12[c]	15
$Cu(OTf)_2$	5.69	9.6[a]	16
ZIF-68	8.96	10.2[a]	17
ZIF-69	11.2	10.08[a]	17
Ni-MOF	17.92	26.56[a]	18
ZIF-8	4.48		19
MIL-101- Cr	14.56 (293 K)	36.65[a] (293 K)	20
Cu(MOF)	10.53	22.57[a]	21
$Cu(INA)_2$	17.90	40.16[c]	22
Al-BDC	16.31	11.9[c]	22
Ni-HKUST-1	37.49	20.56[a]	23
Boron nitride	14.78	32[a]	24
$[Ni_3(HCOO)_6]$	18.37	30.9[c]	25
ATC-Cu	64.96	40.9[a]	26
ROD-8	17.16	25.7[a]	27
Zeolite 5A	22.62		28
$Ni(OAc)_2L$	25.76	40.1[a]	28
Al-CDC	32.06	82[a]	This work
Al-CDC		81.3[c]	This work
In-CDC	14.02	68[a]	This work
In-CDC	14.96	71[a]	This work

[a] Calculated using IAST selectivity. [b] Calculated using mixture selectivity. [c] Calculated using selectivity obtained from Henry's law selectivity.

References

[1] F. Niekiel, M. Ackermann, P. Guerrier, A. Rothkirch, N. Stock, *Inorg. Chem*. **2013**, *52*, 8699-8705.

[2] H. Kumagai, M. Tanaka, K. Lnoue, K. Takahashi, H. Kobayashi, S. Vilminot, M. Kurmoo, *Inorg. Chem.* **2007**, *46*, 5949-5956.

[3] L. Wang, T. Song, C. Li, J. Xia, S. Wang, L. Wang, J. Xu, *J. Solid State Chem.* **2012**, *190*, 208-215.

[4] K. Yao, Y. Chen, Y. Lu, Y. Zhao, Y. Ding, *Carbon* **2017**, *122*, 258-265.

[5] J. Bachman, D. Reed, M. Kapelewski, G. Chachra, D. Jonnavittula, G. Radaelli, J. Long, *Energy Environ. Sci.* **2018**, *11*, 2423-2431.

[6] S. Rege, R. Yang, *Sep. Sci. Technol*. 2001, *36*, 3355-3365.

[7] Y. Bae, R. Snurr, *Angew. Chem. Int. Ed.* **2011**, *50*, 11586-11596.

[8] Y. He, R. Krishna, B. Chen, *Energy Environ. Sci*. **2012**, *5*, 9107-9120.

[9] M. Tong, Q. Yang, Q. Ma, D. Liu, C. Zhong, *J. Mater. Chem. A*. **2016**, *4*, 124-131.

[10] L. Li, , L. Yang, J. Wang, Z. Zhang, Q. Yang, Y. Yang, Q. Ren, Z. Bao, *AIChE J*. **2018**, *64*, 3681-3689.

[11] M. Rivera-Ramos, A. Hernández-Maldonado, *Ind. Eng. Chem. Res*. **2007**, *46*, 4991-5002.

[12] X. Ren, T. Sun, J. Hu, S. Wang, *Micropor. Mesopor. Mater*. **2014**, *186*, 137–145.

[13] J. Möllmer, M. Lange, A. Möller, C. Patzschke, K. Stein, D. Läassig, J. Lincke, R. Gläser, H. Krautscheid, R. Staudt, *J. Mater. Chem.* **2012**, *22*, 10274-10286.

[14] P. Nguyen, H. Nguyen, H. Pham, J. Kim, K. Cordova, H. Furukawa, *Inorg. Chem*. **2015**, *54*, 10065−10072.

[15] D. Saha, Z. Bao, F. Jia, S. Deng, *Environ. Sci. Technol*. **2010**, *44*, 1820-1826.

[16] X. Wang, L. Li, J. Yang, J. Li, *Chin. J. Chem. Eng*. **2016**, *24*, 1687–1694.

[17] B. Liu, B. Smit, *J. Phys. Chem. C*. **2010**, *114*, 8515-8522.

[18] X. Liu, Y. Guo, A. Tao, M. Fischer, T. Sun, P. Moghadam, D. Jimenez, S. Wang, *Chem. Commun*. **2017**, *53*, 11437-11440.

[19] J. Prez-Pellitero, H. Amrouche, F. Siperstein, G. Pirngruber, C. Nieto-Draghi, G. Chaplais, A. Simon-Masseron, D. Bazer-Bachi, D. Peralta, N. Bats, *Chem. Eur. J*. **2010**, *16*, 1560-1571.

[20] Y. Zhang, W. Su, Y. Sun, J. Liu, X. Liu, X. Wang, *J. Chem. Eng. Data*. **2015**, *60*, 2951-2957.

[21] X. Wu, B. Yuan, Z. Bao, S. Deng, *J. Colloid Interface Sci.* **2014**, *430*, 78-84.

[22] J. Hu, T. Sun, X. Liu, Y. Guo, S. Wang, *RSC Adv*. **2016**, *6*, 64039–64046.

[23] X. Jia, N. Yuan, L. Wang, J. Yang, J. Li, *Eur. J. Inorg. Chem.* **2018**, *2018*, 1047–1052.

[24] D. Saha, G. Orkoulas, S. Yohannan, H. Ho, E. Cakmak, J. Chen, S. Ozcan, *ACS Appl. Mater. Interfaces*. **2017**, *9*, 14506-14517.

[25] Y. Guo, J. Hu, X. Liu, T. Sun, S. Zhao, S. Wang, *Chem. Eng. J*. **2017**, *327*, 564–572.

[26] Z. Niu, X. Cui, T. Pham, P. Lan, H. Xing, K. Forrest, L. Wojtas, B. Space, S. Ma, *Angew. Chem. Int. Ed*. **2019**, *58*, 10138-10141.

[27] R. Li, M. Li, X. Zhou, S. Ng, M. O'Keeffe, D. Li, *CrystEngComm*. **2014**, *16*, 6291–6295.

[28] C. Kivi, B. Gelfand, H. Dureckova, H. Ho, C. Ma, G. Shimizu, T. Woo, D. Song, *Chem. Commun*. **2018**, *54*, 14104—14107.